

## **Integration of Aeromagnetic Data and Landsat Imagery for structural Analysis for discovery of Kimberlites in parts of Eastern Dharwar Craton**

G. Ramadass\* , A. Subhash Babu \*\* and M. Preeti \*

\*Center Of Exploration Geophysics, Department Of Geophysics, Osmania University, Hyderabad.

\*\* RMSI Private Limited Auriga, Hyderabad.

---

**Abstract:** *In this study, different digital format data sources including aeromagnetic and remotely sensed (Landsat 8 and ASTER) images were used for structural and tectonic interpretation of the Mahabubnager and Gulbarga districts of Telangana and Karnataka states in the Eastern Dharwarcraton. From analysis of Landsat and ASTER images, the surface morphology and major lineaments trending in the NW-SE, E-W and NE-SW were identified. Qualitative analysis of IGRF corrected aeromagnetic data were carried out using the analytical signal, reduction to pole, horizontal & vertical gradient maps, several lineaments trending in three major directions NE-SW, NW-SE and E-W were delineated. The structural features inferred from image analysis were corroborated, the zones of intersection of these structural trends which could have acted as potential sites for kimberlites emplacement were accordingly delineated at 21 locations. Subsequently, quantitative analysis of magnetic inversion at 21 profiles are carried out utilizing GM-SYS and Geosoft software, brought out the subsurface configuration of kimberlites. The inferred magnetic models are exhibiting V-shaped / Oval type structure. Depth of the inferred structures has been revealed by the Euler deconvolution methods suggest depth varies from 536 to 1640 mts.*

**Keywords:** *Kimberlites, Lineaments, Deconvolution, Aeromagnetic Data, domal structures, drainage pattern.*

---

### **I. Introduction**

An integration of Landsat and Aeromagnetic investigations are very well known in a wide range of geological and exploration studies and they play a very significant role in demarcating the lithological contacts, local and regional geological structures. It provides data on a broad scale of structural features like deep seated fault/fracture corridors, domal structures, disjunction zones, radial fractures, linear grabens, lineaments and resultant structural features formed due to emplacement of dioptric granites, deep crystalline basement as well as the occurrence of volcanic rocks.

In this study, several digital image -processing techniques were used to enhance the ability to structural interpretation of Landsat 8 & ASTER images. These methods were integrated with airborne geophysical exploration methods using Aeromagnetic techniques. Aeromagnetic lineaments are usually identified with faults, all the magnetic lineaments are not alike. A proper classification of these lineaments reveals a wealth of structural detail. Therefore, geophysical detection of kimberlite and related rocks involving contrasts in physical properties such as magnetic susceptibility contrasts between kimberlites and their host rocks has been used [1] and [2]. Several studies have been reported over the study region [3] and few academic publications were available on the Narayanpet Kimberlite Field (NKF) are restricted to Narayanpet, Maddur and Kothakota areas. About Bhima Kimberlite Field, published literature is scanty. Some of the authors [4],[5],[6],[7],[8],[9],[10],[11]&[12] through some light on adjacent areas.

An attempt is made here to obtain magnetic interface/structure and a clearer perception of the structural configuration and to find any possible correlation between the kimberlites occurrences using high resolution aeromagnetic data and compare them with the surface lineaments deduced from analysis of Landsat imagery data.

### **II. Data Base**

The current study area was covered under a national program of aeromagnetic survey was organized by the Geological survey of India (GSI) to cover the entire country by systematic Multi-sensor Twin Otter Airborne geophysical surveys systems (TOASS) were carried out by AMSE wing of GSI During 2001-04, about 12,940 sq km. Aeromagnetic collected with NE-SW oriented flight lines direction and clearance of 120m (AGL), 500m mean flight line spacing. Contour Interval 10nT Mean Inclination 19.33° Mean Declination -1.353° and Mean Total Field of 41528.9nT IGRF corrected data in the scale of 1:50,000 purchased from Airborne mineral Surveys and Exploration wing (AMSE) of GSI. The study area lies in-between geographic coordinates of 16° 50' 25"N, 77°04' 41"E and 16° 29'39"N, 77° 35' 26"E and falls in parts of the Survey of India (SOI) 1:50,000 scale

topo sheets of 56 H1,2,3,5,6,7,9,10 and 11. The total area is about 1933 sq. km. Study area covered two towns those are Narayanpet of AP and Yadgir of Karnataka (Figure 1), which are well connected with state high-ways to major cities. Narayanpet is connected by road about 165 km distance and Yadgir is connected by road about 210 km distance from Hyderabad. Narayanpet Road and Yadgir railway stations are on Chennai-Mumbai rail route. The standard data product for the area of interest corresponds to Landsat 8 scenes with path-row numbers of 144-48 and 144-49 images were acquired on 29<sup>th</sup> April 2013 and 145-48 image was acquired on 6<sup>th</sup> May 2013.

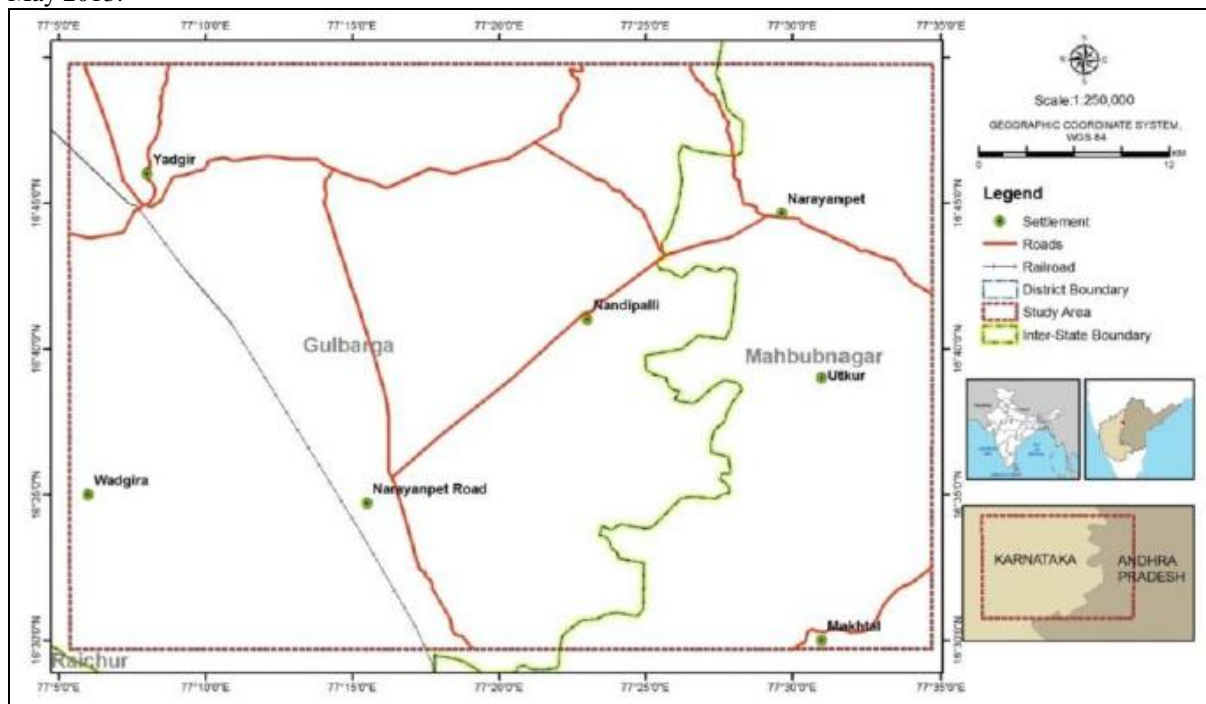


**Fig.1:** Location of the Study Area.

### Geology And Tectonics

Geologically, its character is typical falling under Archean –Precambrian Eastern Dharwar craton. The Dharwar craton is considered to consist of two distinct geological sub-cratons, the older western Dharwar craton and the eastern Dharwar craton [13]. The Narayanpet region is characterized by crustal deformation and forms a type area for the eastern sub-craton [9]. Where theleotitic and komatiitic meta-basalts and felsic volcanic formed 2700 million years ago [14],[15]. The area mainly consists of granite and gneisses, where synformal keels, rafts and enclaves of meta-supra crustal rocks of Gadwal schist belt comprising ultramafic amphibolites, meta-basalts and quartz-sericite schist of Archean-Proterozoic age trending NW – SE direction occur in the north, the belt is concealed under Deccan trap cover and in the south it disappears under the Proterozoic rocks of Cuddapah basin [3]. A number of NW-SE, E-W and NE-SW trending intrusive dykes are a geologically distinctive feature of the area.

The geology of Narayanpet area shown in Figure 2 [16], north of Krishna River is represented by grey granite and gneiss with minor pink feldspar bands representing the Peninsular Gneissic Complex (PGC). The zone east of Yadgir is marked by metabasic schists and amphibolites bands within the PGC as basic enclaves. Narayanpet Kimberlite Field (NKF) is characterized by two main fracture domains: an E-W trending strike slip fault associated NE-SW trending fractures in the Maddur-Kotakonda area, and a predominantly E-W trending strike-slip fault set with associated NNW-SSE trending fractures west of Narayanpet. All the known kimberlites of the NKF are located either along the E-W trending faults or at their intersection with the NNW-SSE trending or NE-SW trending fractures [17]. All the kimberlites of NKF are emplaced into migmatitic gneisses, and granitoids.

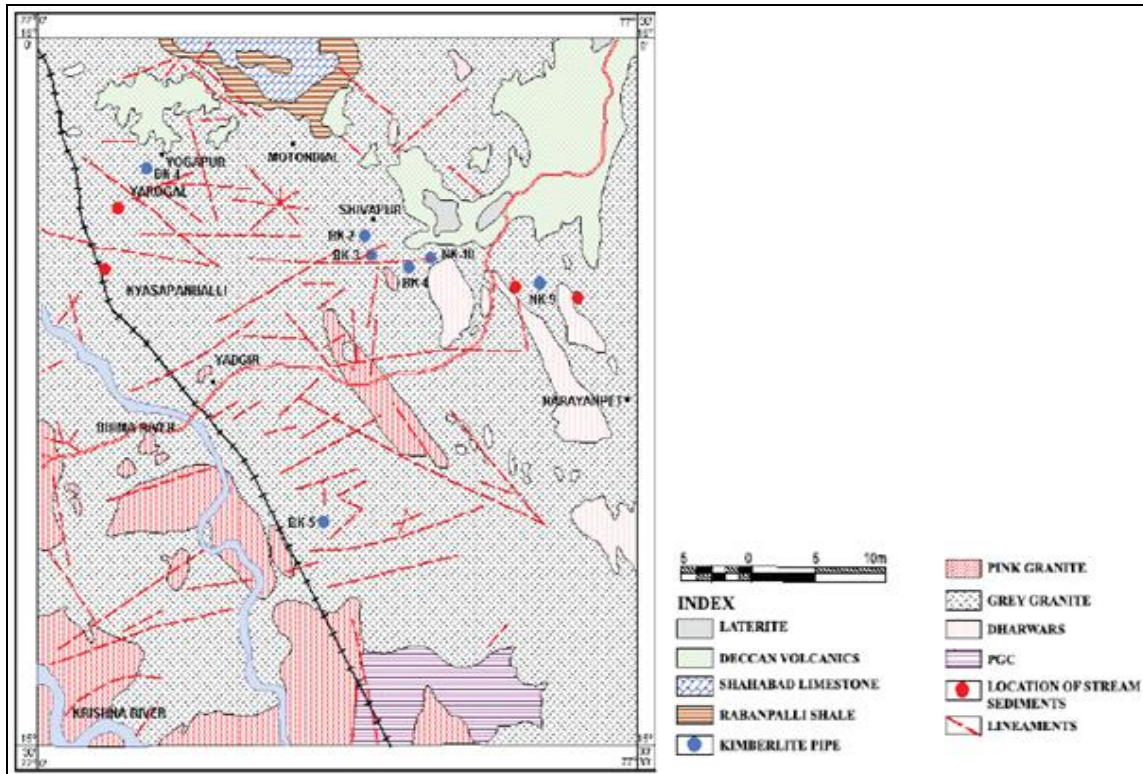


Fig.2: Geological Map showing Narayanpet Kimberlite Field (NKF) (after GSI, 2011).

### Landsat 8 And Aster (Etm<sup>+</sup>) Analysis:

Structural discrimination has been done with various spectral geological techniques using Landsat 8 and ASTER (Figure 3 and Figure 4) satellite images. Various types of FCC image were prepared using several band combinations and as many band rationing/ indexing techniques mentioned by several authors [18],[19],[20],[21],[22] were used to correlate the available geological structures of the study area as well as to find new litho-units of the study area.

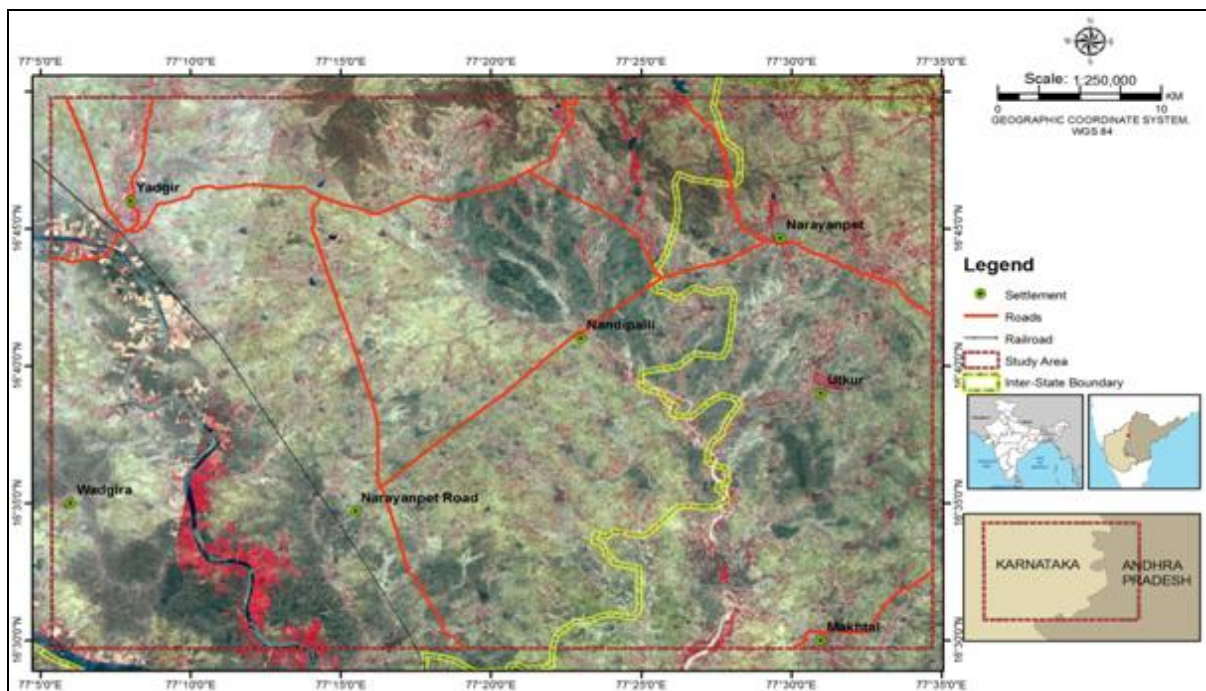
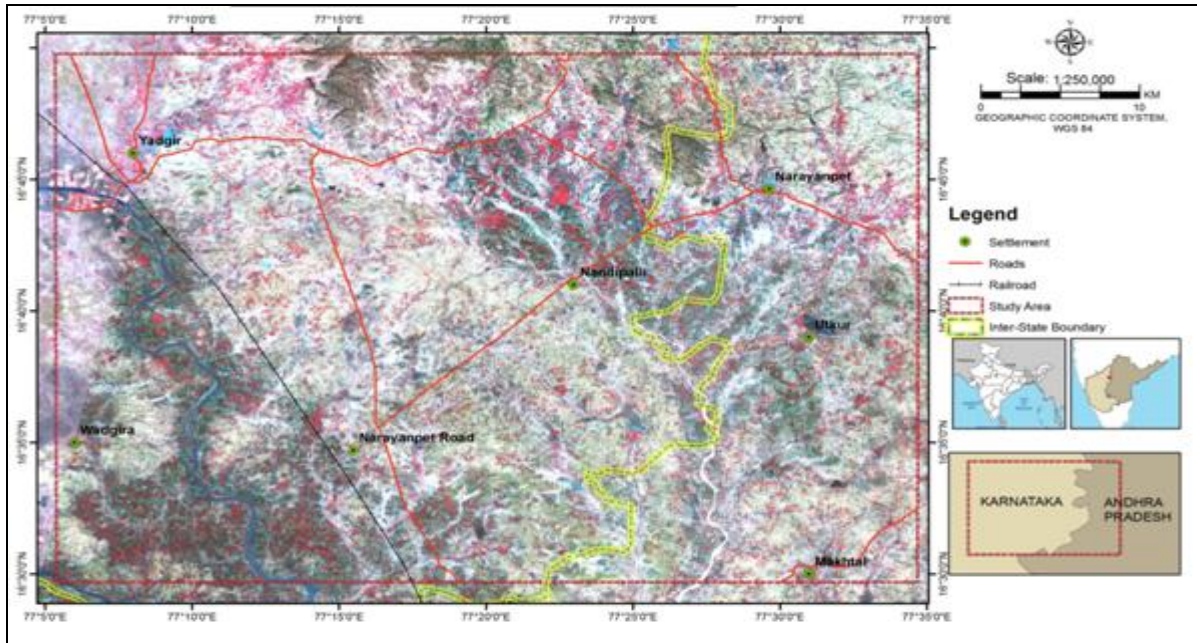


Fig.3: Landsat 8 satellite image of the Study Area.



**Fig. 4:** ASTER satellite image of the Study Area.

New version of ERDAS 10.1 and ENVI 5.0 software were performed to clip the satellite images, enhance, manipulate, display and process raster, as well as vector data for the study area. Various visual interpretation of the satellite image was carried out after the pictorial quality of the image was improved through linear enhancement and filtering of the image. Automated lineament extraction techniques was used to increase the details of existing data of structural and geological maps.

Geologically all faults, folds, joints, fractures etc are considered to be as lineaments. The drainage of the area is easily visible in the Landsat 8 and ASTER images. These can be identifiable through remote sensing using lithological displacement, drainage pattern which follows faults (e.g. Trellis drainage pattern), bedding planes, folds which could be identifiable through its lithologic similarities in the curvilinear beds, fault scarps, emplacement of dykes through fault planes, weathering pattern through joints (e.g. columnar joints in basalts) etc. Many studies have emphasized the importance of lineament interpretations and digital lineament analysis in localizing the major mineral deposits and notes that there is a strong correlation between mineral deposits and lineaments [23],[24],[25],[26].

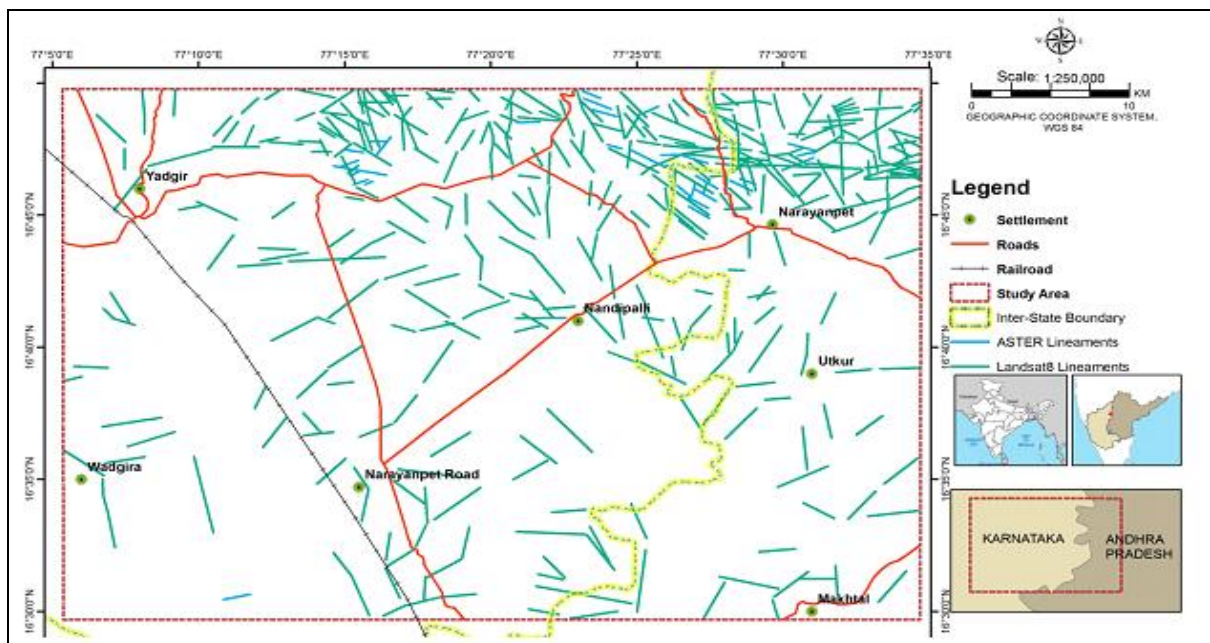


**Fig. 5:** ASTER and Landsat 8 derived Lineaments of the Study Area.

In the present study, visual interpreted lineaments using satellite images both Landsat 8 and ASTER reveal that these lineaments densities are very high at north and north-east of the study area, where the high lands are there (Figure 5).

Prominent linears inferred from the Landsat imagery, trending NW-SE, ENE-WSW, NE-SE and N-S directions are shown in Figure 5. These lineaments of the high lands are mainly joints and fractures rather than faults. In buried piedmonts where granitic rocks with little soil cover and pediplains where soil cover is much high, these lineaments are not visible much through visual interpretation. The area around Maddur -kotakonda is dominated by the presence of biotite granite associated with ENE-WSW and NW-SE trending features. In the western part, the area to the north and east of Narayanpet is dominated by migmatitic gneiss with schistose patches, and the contact is a fault contact, the E-W trending basement fault kimberlites of Maddur-Narayanpet have affected the sediments of the Cuddapah Supergroup in the east. The inferred NW-SE trending strike slip faults, support for which comes from earlier studies [27],[28] are significant because they comprise the tectonic indicators of kimberlite and Lamproites [29] that are associated with diamonds.

### Morph Structural Analysis

The tectonic disposition of deep seated intersecting lineaments in conjunction with atmospheric forces of weathering and erosion results in corresponding domal geomorphologic structure, such geo-morpho features may characterize kimberlite field localization. Accordingly, it is useful to study the topography and drainage pattern of the region from which the disposition of various geomorphic units can be identified.

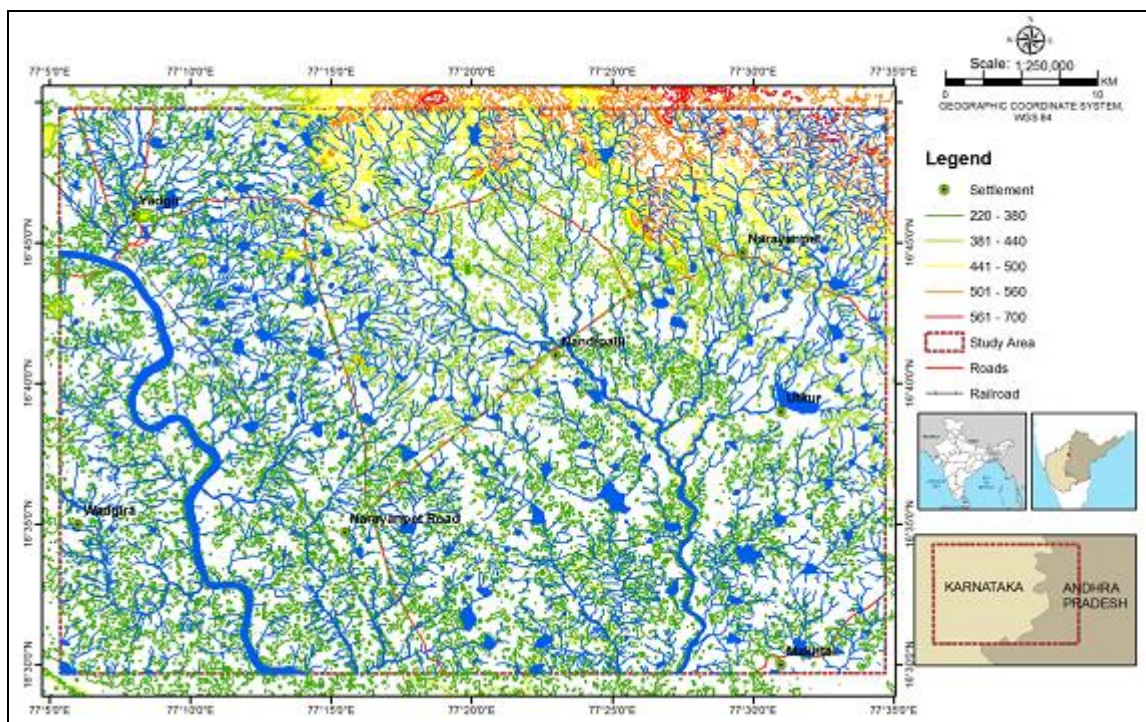


**Fig. 6:** Drainage and water bodies overlaid on contours.

The drainage density map of study falls in toposheet No. 56H/5,6,9 and 10 parts of Mahabubnagar district of Telangana and Gulbarga district of Karnataka states are show in figure 6 varies from a high of over 650 m northwest of Narayanpet and northeast of Mahaboobnagar to low of 280m by the river Krishna east of Gadwal. Drainage is dendritic to sub-dendritic, dendritic homogenous nature of the area and controlled by numerous joints and fractures. The general slope of the area is observed tending towards the southeast. Flood Plains are mainly located along with the Krishna River, which is just passing through the extreme SW of the study area and Bhima River, which is flowing almost NNW to SSE direction in the SW portion of the study area. The Peddavagu is also showing the flood plains in the study area even through this stream is dry throughout the year except few days after rains.

The terrain represents a gentle undulatory plain with few dissected hills in the north and inselbergs of granitic rocks many places in a scattered manner. The highest elevation is 639 about 8.6 km North East of Narayanpet town, Krishna River passes through extreme south – east corner of this study region. Bhima river, one of major tributary of Krishna river is flowing in the south-west portion of the study region.

Alluvial or Pediplains areas are adjacent to both Krishna and Bhima river plains where cultivation is going-on during rainy season. Adjacent to some of the minor streams also alluvial plains are seen in the study area. The material transported to these areas is mainly block soil, eroded from Deccan Traps, where these are available in the west and north of the study area.

Domal structures are reflected in the geomorphology of the region as elevated circular features, the remote sensing approach to locate potential kimberlites zones is to delineate region of domal geomorphology that is characterized by topographic highs. Topographic highs in turn are indicated by regions of circular or radial alignment of the drainage. The general slope of the area is observed tending towards the southeast.

### Qualitative Analysis Of Aeromagnetic Data

Figure 7 is the contoured IGRF corrected Total Magnetic Intensity of the study area, contoured with an interval of 10nT. Aeromagnetic anomaly map has brought out the disposition of various litho-units and structural fabric of the area. The magnetic signatures range from a low of -150nT along western region of the study area, to a high of 550nT in the south-western and north-eastern parts of the region, high magnetic trend is almost near the confluence of Krishna and Bhima rivers as well as north-eastern highlands (north of Narayanpet town).

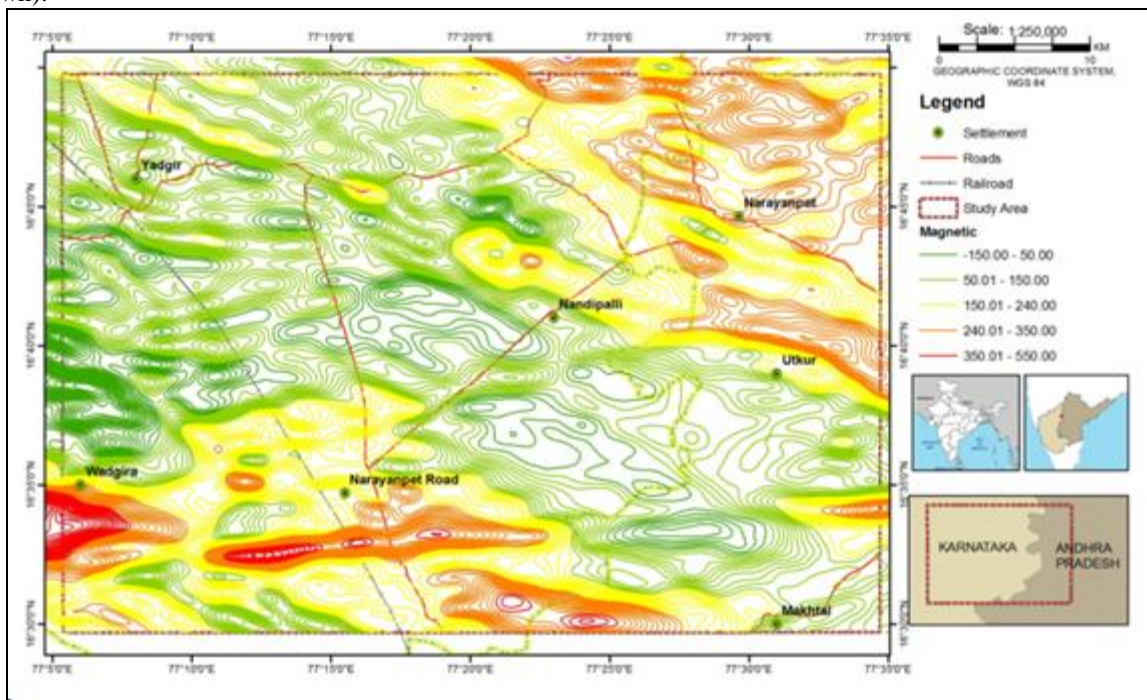


**Fig.7:** Total Magnetic Intensity (TMI) contours of the Study area.

Figure 7 shows the distinct pattern of highs and lows, at some places steep gradients between them are describes as prominent magnetic lineaments. Which are attributable to the complex assemblage of features of varied dimensions and directions from different phases of magmatic activity. Some of the features are associates with basic/ultra basic/younger acidic intrusive that indicate zones of magnetic permeability [28].

While comparison of the magnetic signatures with geology of the region not many inferences are made because the various forms of granites (migmatites, gneisses, pink / grey granites and /or biotite granites) are magnetically not much distinctive. The magnetic highs and lows are in conjunction of subsurface faults in the granitic terrain. Not with the composition of the granites, the study area covers various forms of granites along with little Dharwar schist. Few basic/ ultra basic dykes are available as intrusive rocks. A NW-SE trend to NE-SW trends of fault axes are evident in highs and lows in figure 7, two other trends of magnetic high responses are also running in the same direction.

Interesting features observed in this area are intersections of NW-SE, E-W, NE-SW and N-S magnetic linear features which are supposed to be intersection of faults. These features are prognosticated kimberlite emplacement at 21 places (AA1, BB1to BB5, CC1 to CC2, DD1 to DD2, EE1, FF1, GG1 to GG3, HH1 to HH3 and II1) in the study region shown in Figure 13. Three E-W and NW-SE aeromagnetic linears are in good correlation with the lineaments identified from the Land sat Imagery.

**Reduction To Pole (RTP)**

The shape of a magnetic anomaly depends on the shape of the causative body. But unlike a gravity anomaly, a magnetic anomaly also depends on the inclination and declination of the body’s magnetization, the inclination and declination of the local earth’s magnetic field, and the orientation of the body with respect to magnetic north. To simplify anomaly shape, [30],[31] proposed a mathematical approach known as reduction to the pole. This method transforms the observed magnetic anomaly into the anomaly that would have been measured if the magnetization and ambient field were both vertical as if the measurements were made at the magnetic pole. This method requires knowledge of the direction of magnetization, often assumed to be parallel to the ambient field, as would be the case if remnant magnetization is either negligible or aligned parallel to the ambient field. The computed reduced to pole values of the study area is shown in Figure 8.

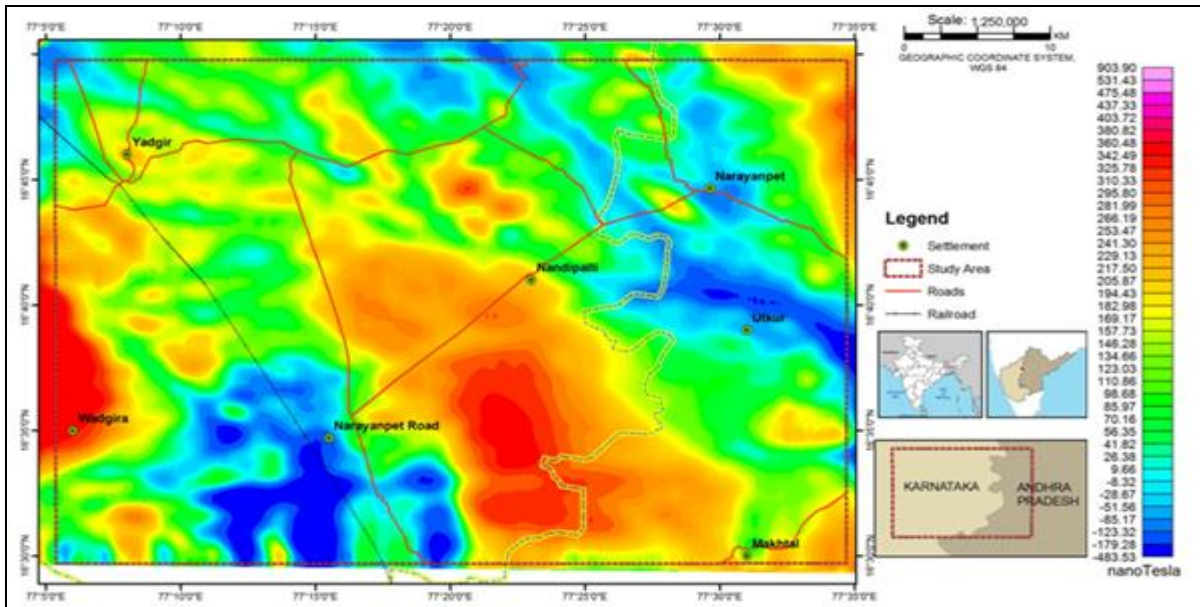


**Fig.8:** Reduced to pole image of the Study area.

**Horizontal, Vertical And Total (Analytical) Gradients**

Gradient maps help define geological contacts more sharply contour maps as also give an estimate of the depth of the source body and the location and dip of its edges. Horizontal gradients of magnetic anomalies are clearly noticed over edges of tabular bodies. For near surface bodies with near-vertical contacts, the maximum horizontal gradient of magnetic as measured along the profile will occur nearly over the contact [32].

The horizontal, first vertical gradients and analytical signal of the aeromagnetic data was calculated using Geosoftpacage (2000) and the results are incorporated into GIS environment.

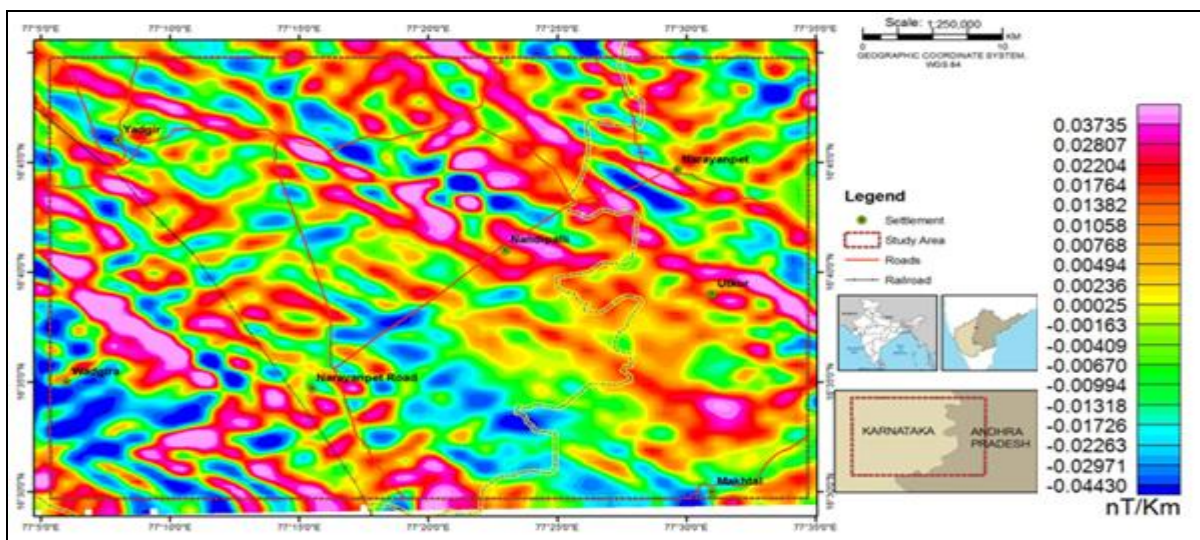


**Fig.9:** Horizontal Derivative (X Direction) Map of the Study Area.

The horizontal gradients along the X direction shown in Figure 9, represent the rate of change of the magnetic field in the corresponding directions that is the X - gradient highlights anomalies with large components disposed along the X-axis. It displays detailed information about the structures, contacts and the tectonic setting of the study area. However, in the study region shows varying trends NW-SE, NE-SW and E-W. Vertical derivatives, on the other hand are based on the concept that the rate of change of magnetic field is much more sensitive to Therefore such maps constitutes a useful technique for demarcation of geological boundaries, details of which are obscured in the original map. Figure 10 is a plot of the vertical derivative of the total magnetic intensity of the study region. This map is dominated by essentially NW-SE and NE-SW striking anomalies. Most of the highfrequency anomalies seen in the vertical derivative map.

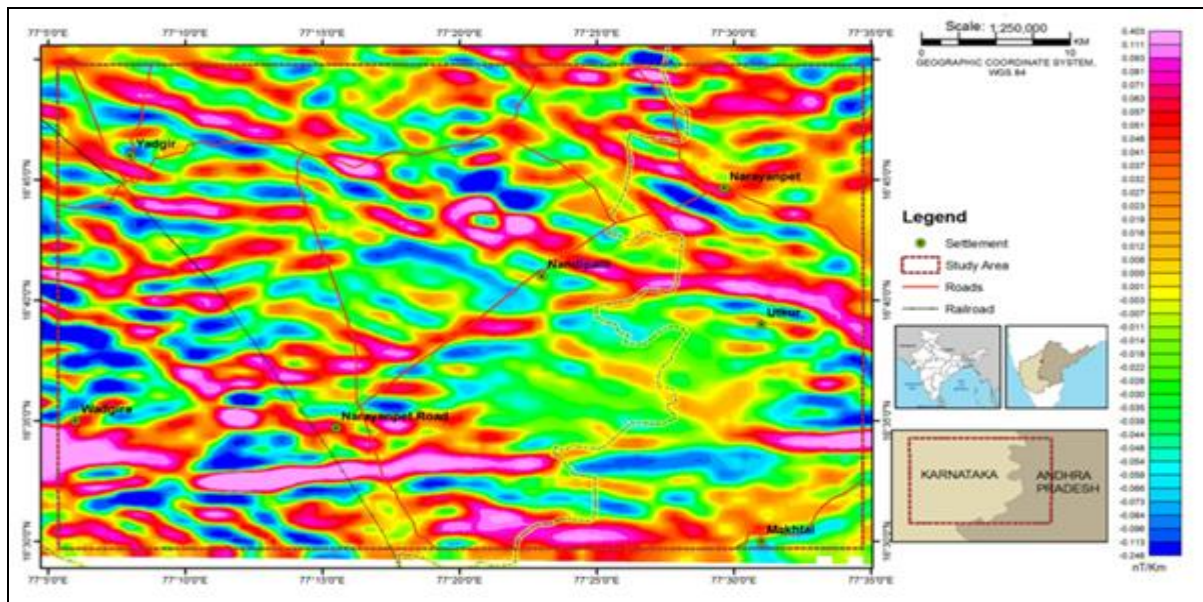


**Fig.10:** First Vertical Derivative Image of the study area.

The analytical signal (Total gradient) (Figure 11) gives finer resolutions of magnetic anomaly trends and locations and disposition of causatives [33] the anomaly square root of the [34] sum of squares of the horizontal (X) and vertical derivatives (Z) along the orthogonal axes of the anomaly resolves the anomaly maps. It encompasses information of the magnetic field variation along the orthogonal axes completely defining it. Consequently, structural features and boundaries of causative sources are determined more accurately.

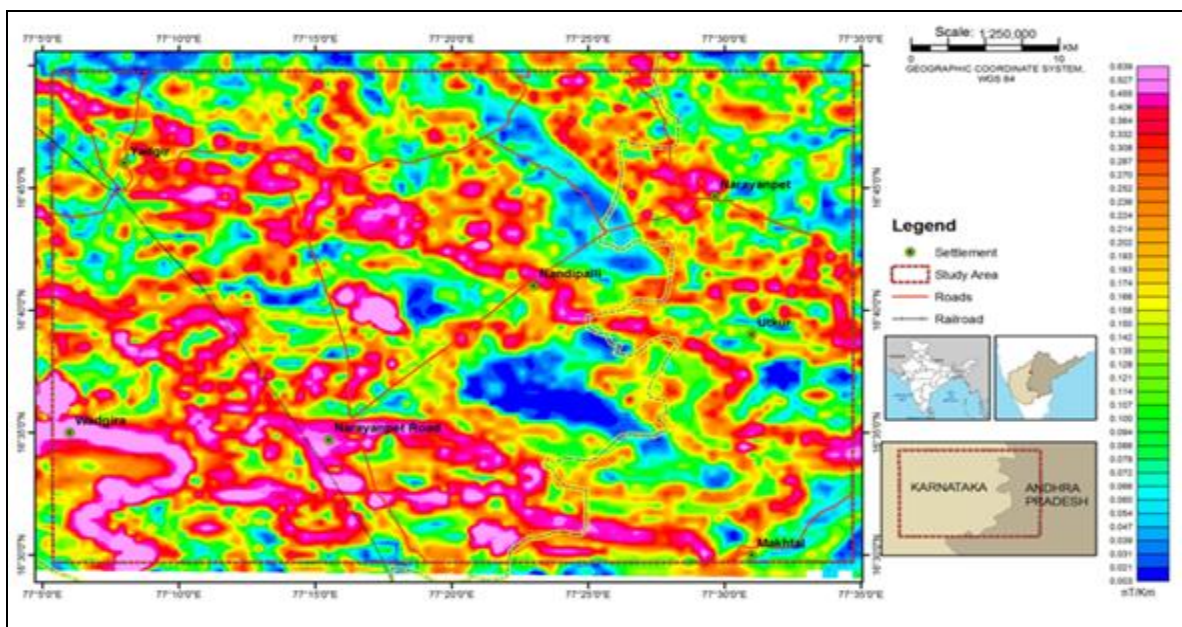


**Fig.11:** Analytical signal image of the study area.

Most kimberlites have a distinctive aeromagnetic signature—in general, a roughly circular anomaly. However, at ground level the anomaly is more complex, and it can have internal highs or be elongated. Typical examples are given by [35] and [1]. Kimberlite magnetic susceptibility is variable and can be as high as  $6 \times 10^{-2}$  SI [36]. Remanence may or may not be present, for instance, many of the kimberlites have a reversed magnetization [37]. In addition, magnetic susceptibility can vary within a given kimberlite pipe [38]. [35] show how aero-magnetic data can be used to identify previously unknown kimberlites; their approach is to look for small, circular, isolated magnetic anomalies.

[39] opined that the typical kimberlite pipe magnetic signatures are roughly equi-dimensional. These anomalies are generally associated with structural features such as faults (linear lows) or diabase dykes (magnetic highs). Kimberlite is generally more susceptible than the surrounding rocks and the total field anomalies can directly indicate the location and shape of tephra fans (amplitude 300nT) or the location of multiple vents in a larger complex (amplitude 60nT). Crater facies kimberlite responses are often expressed as 60 to 150nT smooth magnetic low. In some fields kimberlite pipes are associated with dipolar or strongly negative anomalies reflecting remnant magnetism (amplitude - 800nT and amplitude - 300nT). Unfortunately a large variety of features can produce magnetic anomalies similar to those of kimberlite pipes. Magnetic field lows similar to those generated by some crater facies kimberlite targets are created by deep bedrock topographic depression filled with non-susceptible sediments like clays. Fault intersections are often recessive zones of persistence vertical alteration which generate magnetic lows. Boulder trains of magnetically susceptible bedrock can generate tempting elliptical magnetic highs.

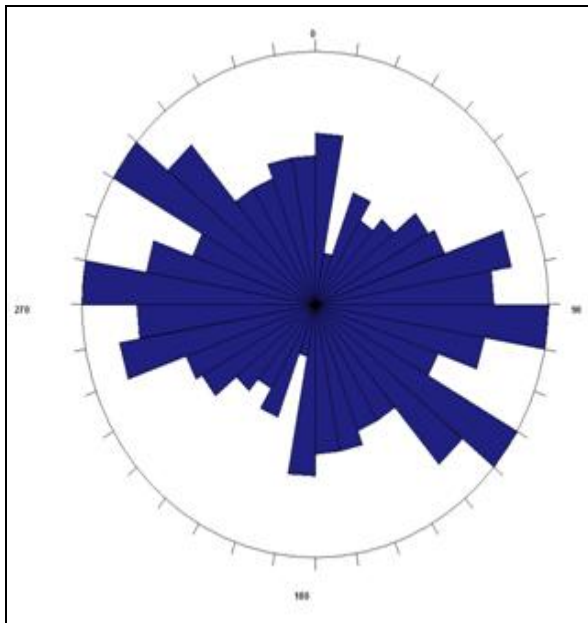


**Fig. 14:** Top Rose diagram showing WNW-ESE and NW-SE trend in the east of Narayanpet (surface lineaments derived from satellite images).

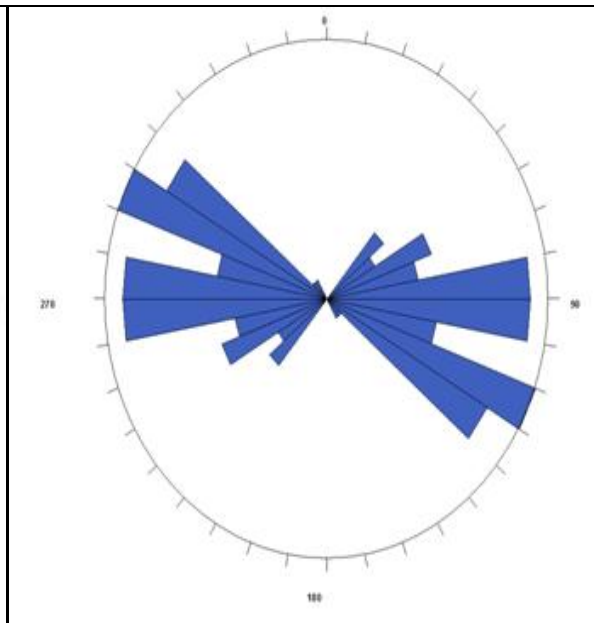


**Fig. 15:** Rose diagram showing WNW-ESE and E-W trend in the W and SW of Narayanpet (deep seated Magnetic lineaments).

### Quantitative Analysis

Though there are many ways to attempt quantitative estimates of depth to an intracrustal magnetic interface. Therefore, in the present studies Modeling /Inversion, sp and Euler deconvolution methods Figure 13 were performed on 21 profiles from AA1, BB1to BB5, CC1 to CC2, DD1 to DD2, EE1, FF1 to FF3, GG1 to GG3, HH1 to HH3 and II of length of up to 10 KM (Figures 12a & 12b).

Depth of the prognosticated kimberlite areas are calculated through Euler Devonvolution Method applied to the IGRF corrected aeromagnetic data to determine the depth of ringcomplex/ cylindrical complex in the study region (Fig.12). The structural Index-2 represents cylindrical shaped body was chosen. Profiles AA1, BB1to BB5, CC1 to CC2, DD1 to DD2, EE1, FF1 to FF3, GG1 to GG3, HH1 to HH3 and III are generated for these prognosticated areas to calculate the same (Figures 12a & 12b) and cross-correlated with profile models (Table 1).

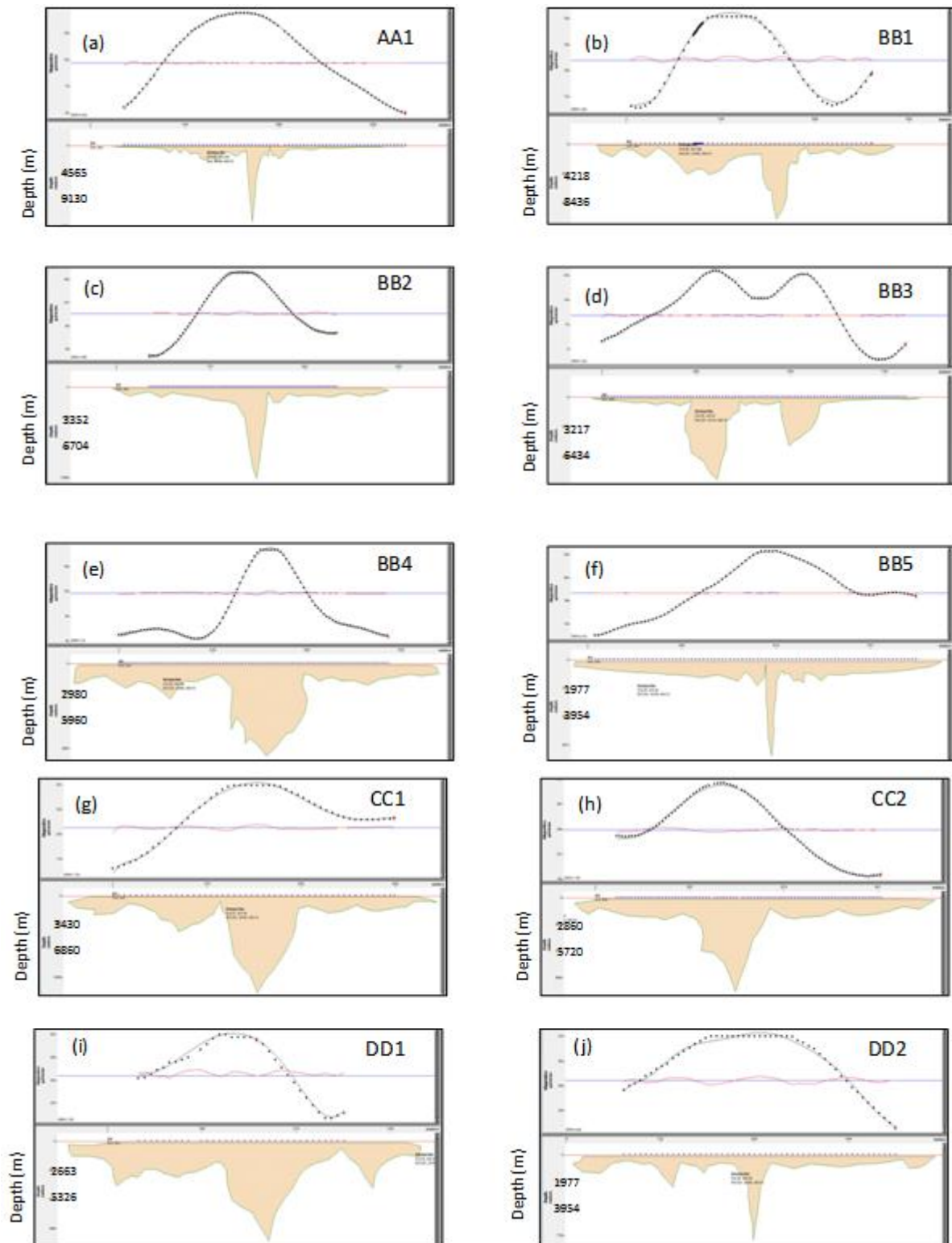


**Fig.12a.:** Inferred Magnetic Interface along profiles  
 (a) AA1 (b) BB1 (c) BB2 (d) BB3 (e) BB4 (f) BB5 (g) CC1 (h) CC2 (i) DD1 (j) DD2

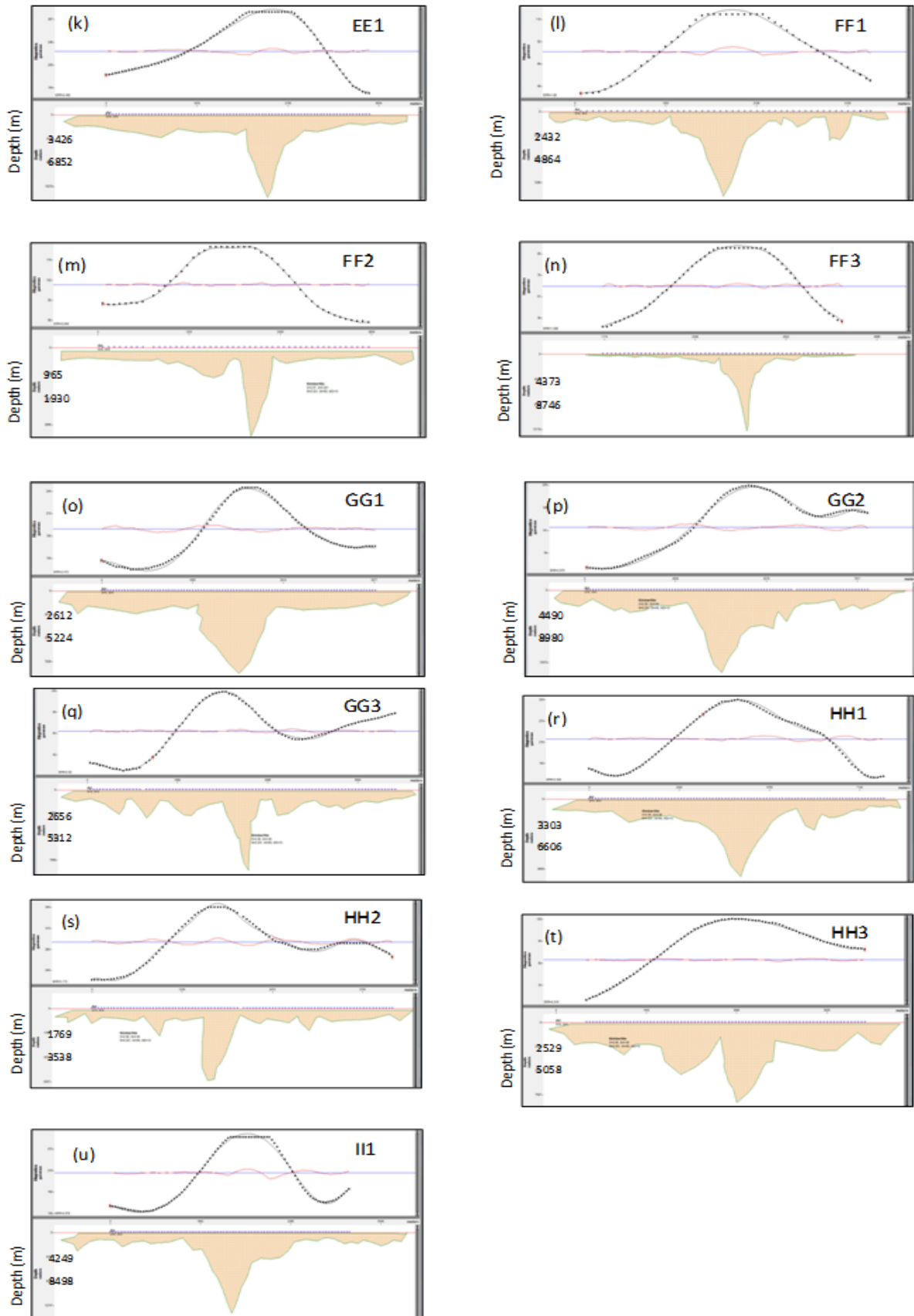


**Fig.12b.:** Inferred Magnetic Interface along profiles  
 (k) EE1 (l) FF1 (m) FF2 (n) FF3 (o) GG1 (p)GG2 (q) GG3 (r) HH1 (s) HH2 (t) HH3 (u) II1

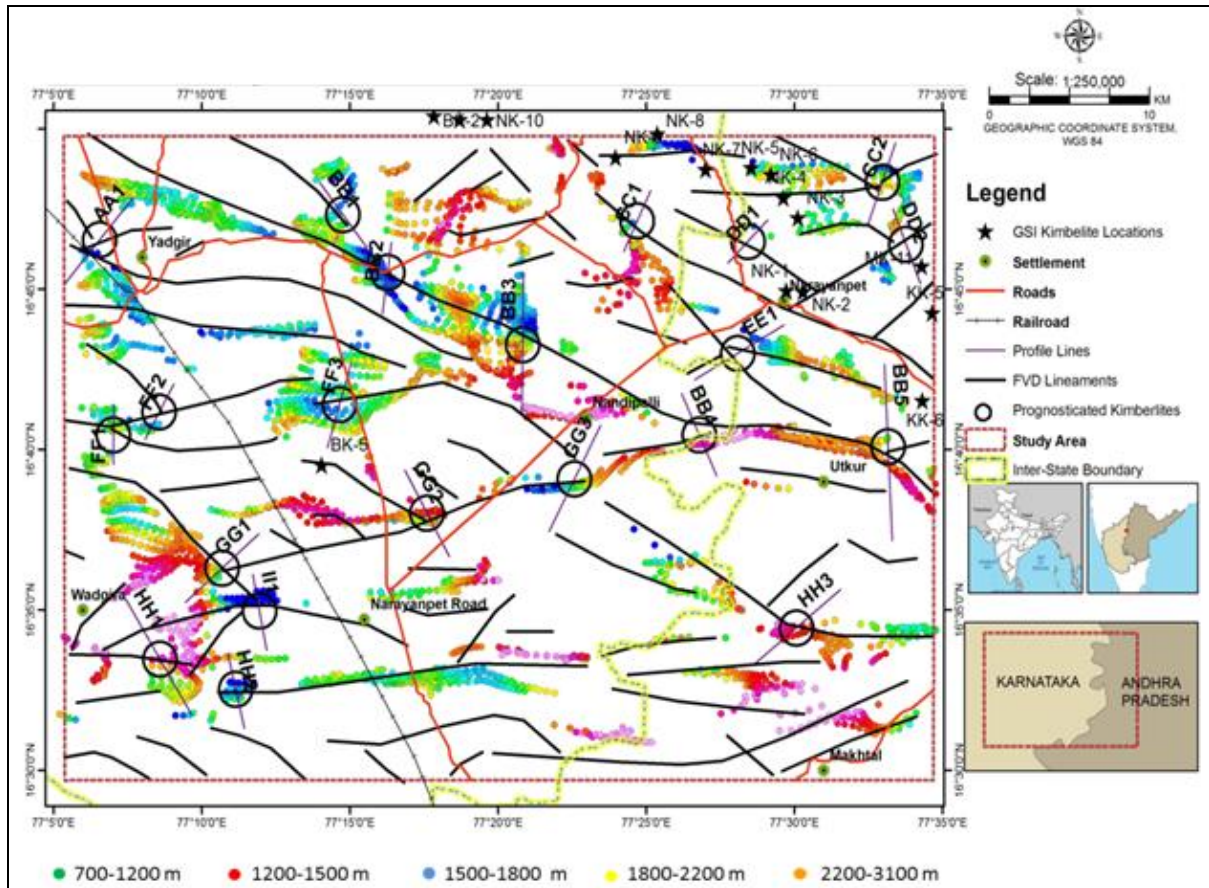


**Fig.13:** Prognosticated Kimberlite locations overlaid on magnetic lineaments, Euler depth solutions (points shown as fill-colored circles) and profile lines.

### Inversion/Modeling

In the present studies Magnetic Inversion is performed using the software GM-SYS (2000), a magnetic modeling software from Northwest Geophysical Associates Inc. This software is based on the methods of [40],[41] make use of the algorithms described in [42]. The software assumes a two dimensional flat earth model and uses the USGS SKI [43], implementation of the Margaret inversion algorithm [44] to liberalize and invert the calculation.

The observed and computed fit of the anomaly as also the inferred magnetic interface along the profiles modeled assuming a two layer (upper and lower magnetic layer based on the magnetic lineament trend) are shown in profiles of AA1, BB1 to BB5, CC1 to CC2, DD1 to DD2, EE1, FF1 to FF3, GG1 to GG3, HH1 to HH3 and II1. For the present investigation a uniform low/high average magnetic susceptibilities of 0.005 cgs obtain from different workers [45] and a remanance of on 0.00175 were assumed for the magnetic layer of the crust. The magnetic inclination and declination for the area taken to be 19.33° and - 1.33° respectively, thus obtained result on in table-1.

From modeled body, magnetic basement layer along these profiles are less than 300 meters all along except at centre of the anomaly. The increase in depth of magnetic basement probably showing the intrusion type oval / carrot shape bodies (Figures 12a to 12b).

**Table -I**

**Prognosticated Kimberlite locations with profiles and depths from various magnetic methods.**

S. No.	Profile	Width of the body in meters	Euler Deconvolution Depths in meters	Magnetic Interface depth in meters	Remarks
1	AA1	250	759	12,989	This is at the intersection of NNW-SSE and E-W (almost) faults. The maximum magnetic response along this profile exhibits 140nT.
2	BB1	200	736	10,699	These profiles are running almost NW-SE to E-W and again NW-SE from north of Yadgir town to east of Utkur village. Total 5 kimberlite pipes are prognosticated in this section. The maximum magnetic response along this profile exhibits 310nT and the minimum response along the fault line is 110nT
3	BB2	300	685	10,070	
4	BB3	2000	699	3,330	
5	BB4	1006	855	13,379	
6	BB5	2000	1640	8,702	
7	CC1	1500	738	8881	These profiles are running E-W and then NE-SW at northeast corner of the study area. The maximum magnetic response along this profile exhibits 340nT and the minimum response along the fault line is 260nT
8	CC2	250	1073	9727	
9	DD1	1500	549	12,214	These profiles are running E-W and running north of Narayanpet town. The maximum magnetic response along this profile exhibits 270nT and the minimum response along the fault line is 220nT.
10	DD2	250	608	9,068	
11	EE1	1250	1223	11,850	This profile is situated at southwest of Narayanpet town. The inferred magnetic interface is 11850 m and the centre 1250 m width, exhibiting the broad v shaped structure; suggest the presence of kimberlitic body.
12	FF1	300	699	10,049	These profiles are running almost WSW-ENE south of Yadgir town. Total 3 kimberlite pipes are prognosticated in this section.
13	FF2	400	765	8,132	
14	FF3	500	768	6,683	
15	GG1	2000	911	15,306	These profiles are running in WSW-ENE north of Narayanpet Road Railway Station parallel to FF1 to FF3. Total 3 kimberlite pipes are prognosticated in this section.
16	GG2	2500	1061	9,122	
17	GG3	921	921	8,401	
18	HH1	1220	1220	9,166	These profiles are running in the direction of E-W parallel to 5 km north of southern border of the study area. Total 3 kimberlite pipes are prognosticated in this section.
19	HH2	648	648	14,103	
20	HH3	400	1631	5,192	
21	II1	400	538	10,957	This profile is situated west of Narayanpet Road. The inferred magnetic interface is 10957 m and in the centre 400 m width, exhibiting the caret type structure, suggest the presence of kimberlitic body.

### III. CONCLUSIONS

From analysis of Landsat - 8 & ASTER (ETM+) satellite images of the Mahabubnager and Gulbarga district of Telangana and Karnataka states regions in the part of the Eastern Dharwar Craton, the surfal configuration were obtained.

The localization of kimberlites is governed by geotectonic controls and / or geomorphologic indicator such as domal geomorphologic structures, structural fabric of the region was elucidated. Four major faults trending in the NW-SE, E-W and NE-SW directions. From the association of reported kimberlite occurrences with domal geological features, a morpho-structural and intersection of lineaments criterion as an interpretation guideline, 21 location were delineated.

A qualitative analysis of aeromagnetic data like reduction to Pole (RTP), Analytical signal. Derivative analysis (vertical and Horizontal) has been performed to anticipate the subsurface structures and rock assemblages, where kimberlites of various geological lineaments (Figure 2, 3 and 4). The structural features inferred from Landsat images were corroborated.

Quantitative analysis of aeromagnetic like Euler deconvolution depth solutions and inversion was performed along a representative 21 profiles across a region associated with kimberlite emplacements to obtain the subsurface structure of the causative body showing V shaped / Oval shape structure, which were found to be localized at intersections of lineaments magnetic interface in the study area.

### Acknowledgement

The authors are grateful to the University Grants Commission (UGC), Govt. of India-New Delhi, for the sanctioning the Emeritus Fellowship of Prof. G. Ramadas and Dean development, Osmania University.

## References

- [1]. Macnae, J.C. 1995. Applications of geophysics for detection and exploration of kimberlites and lamproites. *Journal of Geochemical Exploration*. Vol. 53 (1-3), pp.213-243. Elsevier Science.
- [2]. Power, M., Belcourt, G. and Rockel, E., 2004. Geophysical methods for kimberlite exploration in northern Canada. *The Leading Edge*, Vol.23, No. 11, pp. 1124 – 1129.
- [3]. Ananda Reddy, R.2014. Qualitative Kimberlites analysis of Mafic Dyke Swarms and Kimberlites from Morphological and Geophysical Signatures.NW of Proterozoic Cuddapah Basin, Eastern DharwarCraton.*Journal of the Geological Society of India*. Vol83.March, pp 235-251.
- [4]. Sreerama Murthy, N., Ananda Reddy, R., Livingston, D., Raju, V.L. and Mohan Rao, T. 1997. Geophysical exploration of kimberlite pipes-a case study from Maddur area, Mahboobnagar district, Andhra Pradesh. *Journal of Geophysics*. Vol. 18, pp. 165-174.
- [5]. Sreerama Murthy, N., Ananda Reddy, R., Rao, M.V.R.K., Sunder Raj, B., Murthy, N.V.S. and VittalRao, K.P.R. 1999. A new kimberlite discovery from a structural elucidation of gravity data, Maddur – Narayanpet field, Mahabubnagar district, Andhra Pradesh.*Journal of Geophysics*, Vol. 20, no.1, pp. 3-13.
- [6]. Ramadass, G., Himabindu, D. and RamaprasadaRao, I.B. 2004a. Magnetic basement along the Jadcharla-Vasco transect, DharwarCraton, India. *Current Science*, Vol. 84, No. 11.
- [7]. Ramadass, G., Himabindu, D. and RamaprasadaRao, I.B. 2004b. Magnetic basement of the DharwarCraton in the Precambrian Indian Peninsular Shield. *Current Science*, Vol. 86 (11), pp. 1548-1553.
- [8]. Ramadass, G., Himabindu, D. and Veeraiah, B. 2006a. Morphostructural Prognostication of Kimberlites in parts of Eastern DharwarCraton:Inferences from Remote Sensing and Gravity Signatures. *Journal of the Indian Society of Remote Sensing*, Vol. 34, No. 2. pp. 111-121.
- [9]. Ramadass, G., RamaprasadaRao, I.B. and Himabindu, D. 2006b. Crustal configuration of the Dharwarcraton, India, based on joint modeling of regional gravity and magnetic data. *Jour. Asian Earth Sci.*, Vol.26, pp.437-448.
- [10]. Veeraiah, B., Himabindu, D. and Ramadass, G. 2006. Geological and Structural Inferences from Satellite Image in Parts of the Eastern DharwarCraton, India. *Journal of Indian Geophysical Union*, Vol. 10, No. 3, pp. 255-262.
- [11]. Veeraiah, B., Ramadass, G. and Himabindu, D. 2009. A subsurface Criterion for Predictive Exploration of Kimberlites from Bouguer Gravity in the Eastern DharwarCraton, India.*Journal Geological Society of India*. Vol. 74, pp. 69-77.
- [12]. Mallick, K., Vasanthi, A. and Sharma, K.K. 2012. Bouguer Gravity Regional and Residual Separation: Application to Geology and Environment. Springer.
- [13]. Rajamani V. 1990.Petrogenesis of metbasites from the schist belts of the DharwarCraton Implications in Archaean mafic magmatism. *Jour.Geol.Soc. India* Vol.36.pp 565-587.
- [14]. BalakrishnaS,Rajamani V and Hanson G.N. 1999. U-Pb ages for zircon and titanite from the Ramagiri area, southern India: evidence for the accretionary origin of the eastern Dharwarcraton during the late Archaean.
- [15]. KrogstadE.J,Balakishnan S, Mukhopadhyay D.K, Rajamani V, and Hanson G.n.1989.Plate tectonics 2.5 billion years ago: evidence of Kolar, South India, *Science*, Vol,243,pp1337-1340.
- [16]. GSI. 2011. Detailed information Dossier on Diamond in India. Geological Survey of India. Guha,
- [17]. Rao, K.R.P., Reddy, T.A.K., Rao, K.V.S., Rao, K.S.B. & Rao, N.V. 1998. Geology, petrology and geochemistry of Narayanpetkimberlite field in Andhra Pradesh and Karnataka. *Journal of the Geological Society of India*, Vol. 52, pp.663-676.
- [18]. Goetz, A.F.H. 1975. Application of ERTS images and image processing to regional geologic problems and geologic mapping in northern Arizona, JPL Technical Report 32-1597, Jet Propulsion Laboratory, Pasadena, CA.
- [19]. Chavez, P.S. Jr., Berlin, G.L. and Sowers, L.B. 1982. Statistical method for selecting Landsat MSS ratios, *Journal of Applied Photographic Engineering*, Vol. 8(1), pp. 23 - 30.
- [20]. Singer, R.B. 1980. Near-infrared spectral reflectance of mineral mixtures, systematic combinations of pyroxenes, olivine and iron oxides, PSD Publications.No. 258, MIT, Cambridge, MA.
- [21]. Miller, L.D. and Pearson, R.L. 1971. Areal mapping program of the IBP grassland biome: Remote Sensing of the productivity of the short grass prairie as input into bio system models, 7th Proceedings of International Symposium. *Remote Sensing of Environment*. Vol. 1, pp. 175–205.
- [22]. Price, J.C. 1995. Examples of high resolution visible to near infrared reflectance spectra and a standardized collection for remote sensing studies: *International Journal of Remote Sensing*, Vol. 16, pp. 993–1000.
- [23]. Kutina, J. 1969. Hydrothermal ore deposits in the western United States; A new concept of structural control of distribution, *Science* Vol.165,pp 1113-1119.
- [24]. Katz, M. 1982. Lineament analysis of Landsat imagery applied to mineral exploration. In *Mineral exploration techniques in tropical forest areas*. Edited by Lamining, D.I.C and Gibbs, A.K. *Hidden Wealth*, pp.157-166.
- [25]. Liu, C.C. Sousa M.D.A. Jr and gopinath, T.R. 2000. Regional Structural analysis by Remote sensing for Mineral Exploration, Paraiba State, Northeast Brazil. *Geocarto international*, Vol.15.No.1, pp.70-77.
- [26]. Rein Bert and Kaufman H, 2003. Exploration for Gold using panchromatic stereoscopic intelligence satellite photographs and Landsat, TM data in the Hebei area, China, *International Journal of Remotesensing*, Vol.24, No.12, pp 2427-2438.
- [27]. Nayak, S.S. and Kasiviswanthan, C.V. Reddy, T.A.K and NagarajRao, B .K. 1988. new find kimberlitic rock in Andhra Pradesh near Maddur, Mahabubnagar district, *journal of the Geological Society of India*, pp.521-555.
- [28]. Sinha, P.K., Surendranath, M., De, S.K., Muralidharan, P.K. and Misra, R.S. 2003. A GIS approach in Mineral Targeting with Narayanpet Kimberlite Spatial Dataset. *Map India Conference 2003*.
- [29]. Haggerty, S.E. 1994. Superkimberlites: a geodynamic window to the Earth's core. *Earth Planet. Sci. Lett.* Vol. 122, pp. 57–69.
- [30]. Baranov, V. 1957. A new method for interpretation of aeromagnetic maps pseudo-gravimetric anomalies: *Geophysics*. Vol. 22, pp. 359–383.
- [31]. Baranov, V. and Naudy, H. 1964. Numerical calculation of the formula of reduction to the magnetic pole: *Geophysics*, Vol. 29, pp. 67–79.
- [32]. Dobrin M.B and Savit C.H. 1988. *Introduction to Geophysical Prospecting* 4<sup>th</sup> Edition McGraw-Hill Book Co. pp.867.
- [33]. Ramadass G, 1990. Resolution of gravimagnetic and radiometric signals by Hilbert Transform, *Terra Research*, pp:160-166.
- [34]. Nabighian, M.N., 1972. The analytic signal of two-dimensional magnetic bodies with polygonal cross-section—Its properties and use for automated anomaly interpretation: *Geophysics*. Vol. 37, pp. 507–517.
- [35]. Brummer J.J, Macfadyen, D.A and Pegg, C.C. 1992. Discovery of Kimberlites in the Kirkland Lake Area, Northern Ontario, Canada, Part-I Early Surveys and the Surficial Geology, *Exploration and Mining Geology* Vol. pp 339-350, Part II.
- [36]. Litinskii, 1963. Measurement of magnetic susceptibility in prospecting for kimberlites pipes, *Mining Magazine*, vol.109, pp 137-146.

- [37]. Reed, L.E. 1993. Exploration for kimberlites using magnetic: The Gangue Geological Association of Canada Mineral Deposits Division Newsletter, vol.43, pp 1-2.
- [38]. Mwenifumbo, C.J., Kileen, P.G. and Elliot, B.E. 1998. Borehole geophysical signatures of kimberlites in Canada. *The Log Analyst* Vol. 39, No. 2, pp. 38–52.
- [39]. Power, M. and Hildes, D. 2007. Geophysical strategies for kimberlite exploration in northern Canada. *Geophysical Case Histories*. Paper 89. *Proceedings of Exploration 07: Fifth Decennial International Conference on Mineral Exploration*, edited by Milkereit, B. pp. 1025-1031.
- [40]. Talwani, M., Worel, J.L. and Landisman, M. 1959. Rapid gravity computations for two-dimensional bodies with application to the Mendocino submarine fracture zone. *Journal of Geophysical Research*. Vol. 64, pp. 49-59.
- [41]. Talwani, M and Heirtzler, J.R. 1964. Computation of magnetic anomalies caused by two dimensional bodies of arbitrary shape, in Parks, G.A. Ed., *Computers in the mineral industries, Part 1*. Stanford University Publication. *Geological Sciences*. Vol. 9, pp. 464-480.
- [42]. Won I.J and Bevis M. 1987. Computing the gravitational and magnetic anomalies due to a polygon. *Algorithms and Fortran subroutine*. *Geophysics*. Vol.52, pp 232-238.
- [43]. Webring M. 1985 SAKI. A Fortran program for generalized linear inversion of gravity and magnetic profiles. *USGS Open File Report*. Vol.29, pp 85-122.
- [44]. Margaret, D.W. 1963. An algorithm for least squares estimation of non-linear parameters. *Journal of SIAM*. Vol. 11, pp. 431-441.
- [45]. Ramadass, G., RamaprasadaRao, I.B. and Himabindu, D. 2007. Dharwarcraton: crustal model from regional gravity and magnetic signatures. *Int. Assoc. Gondwana Res. (IAGR) Japan, IAGR Memoir, No.10*, pp.227-232.